DEVELOPMENTAL BIOLOGY **204,** 263–276 (1998)
ARTICLE NO. DB989048

The Cellular Mechanism of Epithelial Rearrangement during Morphogenesis of the *Caenorhabditis elegans* Dorsal Hypodermis

E. M. Williams-Masson,*,† P. J. Heid,‡ C. A. Lavin,† and J. Hardin§

**Molecular Biology Laboratory, †Integrated Microscopy Resource, ‡Biochemistry Department, §Program in Cellular and Molecular Biology and Department of Zoology, University of Wisconsin–Madison, 1117 W. Johnson Street, Madison, Wisconsin 53706*

The mechanism by which epithelial cells rearrange is a process that is central to epithelial morphogenesis, yet remains poorly understood. We have investigated epithelial cell rearrangement in the dorsal hypodermis of the *Caenorhabditis elegans* embryo, in which two rows of epithelial cells rearrange in a morphogenetic process known as dorsal intercalation. The intercalating cells extend basal protrusions which squeeze between their opposing neighbors beneath their adherens junctions. As the intercalating cells move forward, these protruding tips become broader in the anterior–posterior and dorsoventral dimensions, effectively "plowing through" the adherens junctions and forcing an opening for the remainder of the intercalating cell to insert between the contralateral cells. These cell movements are dependent upon intact cytoarchitecture, since the pharmacological disruption of microtubules or actin filaments blocks cell rearrangement. The cells appear to intercalate independently of immediately adjacent neighboring hypodermal cells because dorsal intercalation is not blocked by the ablation of the progenitors for either half of the lateral hypodermal cells or the posterior half of the dorsal hypodermis. This is the first case in which the protrusive mechanism underlying epithelial cell rearrangement has been characterized, and we propose a model describing how epithelial cells rearrange within the confines of an epithelial monolayer, and discuss the mechanisms that may be guiding these directed cell movements.

Key Words: **cell rearrangement; intercalation; epithelial morphogenesis.**

INTRODUCTION

The directed rearrangement of cells in early embryos is a major force driving morphogenesis during vertebrate development. For example, during *Xenopus* gastrulation and neurulation, radial and mediolateral intercalation of mesodermal cells result in the convergence of the marginal zone toward the dorsal midline and its extension along the anterior–posterior axis (Wilson and Keller, 1991; Keller and Tibbetts, 1989). Likewise, Schoenwolf and Alvarez (1989) have shown using quail/chick chimeras that the shaping of the neural plate involves mediolateral cell rearrangement, as well as cell division. Cell rearrangement has also been shown to occur during epithelial morphogenesis in teleost embryos, with cell rearrangement and changes in cell shape being responsible for the narrowing of the enveloping layer margin during teleost epiboly (Keller and Trinkaus, 1987).

Cell rearrangement also plays a critical role in epithelial morphogenesis in invertebrate embryos. During sea urchin gastrulation, cell rearrangements and flattening of the epithelial cells have been shown to account for the dramatic elongation of the archenteron and for closure of the blastopore during secondary invagination (Ettensohn, 1985; Hardin and Cheng, 1986; Hardin, 1989). Changes in cell shape and position also play a role in evagination and elongation of imaginal disks during limb formation in *Drosophila* (Fristrom, 1976; Condic *et al.*, 1991), and convergent extension has been shown to drive *Drosophila* germband extension as well (Irvine and Wieschaus, 1994).

Although the importance of cell rearrangement as a driving force during the morphogenesis of epithelial sheets has been well established, the actual mechanism by which epithelial cells reorganize their cellular junctions has remained unclear, as has the patterning information intercalating cells use to undergo directed rearrangement. The dorsal hypodermis of the *Caenorhabditis elegans* embryo is a convenient model system for studying epithelial cell rearrangement. The formation of the embryonic hypoder-

0012-1606/98 $25.00

mis is a critical process in nematode development because it is the contraction of the hypodermis that causes the embryo to elongate fourfold from its initial ellipsoid shape into the tubular structure of the larva during the morphogenetic process known as elongation (Priess and Hirsh, 1986). The nematode hypodermis arises on the dorsal surface of the embryo approximately 240 min after first cleavage at 25°C and organizes into a monolayer of six rows of cells. This epithelial sheet extends bilaterally around the embryo until the migrating ventral edges meet and form adherens junctions, wrapping the embryo in a contiguous epidermal layer prior to elongation. The two central rows of cells form the dorsal hypodermis, the rows of cells on either side of the dorsal cells form the lateral hypodermis, and the two outermost rows become the ventral hypodermis. As the epithelial sheet wraps around the embryo, the two rows of dorsal cells interdigitate, with each dorsal cell inserting between two cells in the contralateral row of dorsal cells. As the dorsal cells intercalate, their nuclei cross the dorsal midline and migrate mediolaterally to the opposite side of the cell. Soon after enclosure, the dorsal and six ventral hypodermal cells fuse and form the syncytial hypodermis that ultimately forms a majority of the outer covering of the adult nematode (Sulston *et al.*, 1983; Podbilewicz and White, 1994).

In this study we analyze in detail the rearrangement of 20 specific epithelial cells during dorsal intercalation in the embryonic hypodermis of *C. elegans*. We show how rearranging cells redistribute their cellular junctions, and have used pharmacological agents to disrupt the cytoarchitecture that is organized concomitant with dorsal intercalation. Finally, we have ablated the progenitor cells of large sections of hypodermis adjacent to the dorsal intercalating cells to address the role of cell interactions during intercalation, and propose a mechanism by which individual epithelial cells are able to migrate and rearrange within the confines of an epithelial monolayer.

MATERIALS AND METHODS

Antibody staining. Embryos were obtained from gravid hermaphrodites via bleach treatment and attached to slides coated with 0.01% poly-L-lysine and processed for antibody staining by the freeze–cracking method (Sulston and Hodgkin, 1988). The specimens were then incubated at 37°C for 1 h in either a 1:500 solution of MH27 antibody or a 1:10 solution of *mcap 77* antibody (Serotec) and PBST buffer (Sulston and Hodgkin, 1988) + 1% dry milk. (MH27 antibody recognizes a component of the adherens junction and was kindly provided by Dr. B. Waterston, Washington University, St. Louis, MO. *mcap-77* antibody recognizes α-tubulin.) The samples were rinsed in PBST buffer and incubated in either a 1:25 solution of FITC-conjugated goat anti-mouse IgG (MH27) or FITC-conjugated goat anti-rat IgG (*mcap77*) for 30 min at 37°C. The samples were rinsed in PBST buffer, sealed in a drop of Slowfade antibleaching solution (Molecular Probes, Eugene, Oregon) and stored at 4°C. Laser scanning confocal microscopy was used to acquire serial optical sections, and was performed at the Integrated Microscopy Resource, University of Wisconsin.

Nomarski time-lapse videomicroscopy. All microscopy was performed as described in Williams-Masson *et al.* (1997). Briefly, embryos were dissected from gravid hermaphrodites and mounted on a 5% agar pad in M9 solution (Sulston and Hodgkin, 1988). Embryonic development was filmed using 4D microscopy, using a modified version of NIH Image for device control and image acquisition.

BODIPY 558/568 phalloidin staining. Embryos were processed for phalloidin staining as described in Williams-Masson *et al.* (1997) and Costa *et al.* (1997). Briefly, embryos were obtained by bleach treatment and subjected to chitinase-chymotrypsin (Sigma) treatment to remove their eggshells. The embryos were fixed in a formaldehyde/lysolecithin fix solution and then pelleted, rinsed, and resuspended in PBST + BODIPY 558/568 phalloidin (Molecular Probes). After phalloidin staining, the embryos were mounted on frosted ring slides in Slowfade and viewed via confocal microscopy.

Scanning electron microscopy. The embryos were collected from gravid hermaphrodites by bleach treatment and the egg shells were removed by chitinase–chymotrypsin as described above. The embryos were passed through a pulled Pasteur pipet to remove the vitelline membrane and were pipetted onto coverslips that had been subjected to silane treatment (Malecki and Ris, 1992; Ris and Malecki, 1993). The embryos were then fixed in 2% glutaraldehyde and 2% formaldehyde in 150 mM sodium phosphate buffer; 2 mM $MgSO_4$, pH 7.4, and were rinsed in 100 mM phosphate buffer, pH 7.4. The samples were dehydrated through an ethanol series and critical-point dried (Ris, 1985). Samples were coated with 1–2 nm of platinum and viewed using a Hitachi S-900 field-emission scanning electron microscope.

Transmission electron microscopy. Embryos were selected and then isolated in dialysis tubing (Hohenberg *et al.*, 1994) containing M-9 medium (Sulston and Hodgkin, 1988). The selected embryos were transferred to high-pressure freezing (hpf) sample holders filled with 1-hexadecene. The sample holders were transferred to a Balzer HPM 010 high-pressure freezer where the freezing process was completed within 30 ms. The hpf embryos were stored in liquid nitrogen until all the samples had been frozen.

The frozen embryos were transferred under liquid nitrogen to cryovials containing a freeze substitution solvent comprised of 1% osmium in sieve-dried acetone. The cryovials were then placed in a metal block and kept at −80°C for 3 days, slowly warmed to −20°C, and maintained at −20°C for 8 h, and then slowly warmed to room temperature. The freeze-substituted samples were kept at room temperature for 1 h prior to rinsing repeatedly with fresh sieve-dried acetone.

Samples were infiltrated and flat embedded in Epon 812 for conventional TEM imaging. Thin sections (50-nm) were cut on a Reichert Ultracut E Ultramicrotome and poststained with lead and uranium for viewing in a Philips 410 Transmission Electron Microscope at 80 kV.

For the three-dimensional reconstruction of an intercalating cell shown in Fig. 4G, sections were aligned using fiducial landmarks and NIH Image software. The cell outline and junctional domains were then manually outlined and converted into binary images. Three-dimensional reconstructions of the binary images were performed using Macstereology.

Laser ablations. Ablations were performed as described in Williams-Masson *et al.* (1997). Briefly, embryos were mounted as for time-lapse microscopy and individual cell nuclei were ablated using a tunable dye laser pumped via a Laser Sciences VSL-337 nitrogen laser (Bull's Eye, Fryer Co.). Cell identity was determined by lineaging for the C ablations, and for the ABarpp ablations by

using a combination of cell lineaging and comparison to a map of early cell positions. Immediately following the ablation, embryonic development was filmed by 4D videomicroscopy. The GFP seam cell marker was visualized directly using a fluorescein filter on an epifluorescence microscope.

Cytochalasin D and nocodazole experiments. The drug experiments were performed as described in Williams-Masson *et al.* (1997). Embryos were exposed to 1 μg/ml nocodazole or 2 μg/ml cytochalasin D (Sigma).

RESULTS

Changes in the Shape and Position of Hypodermal Cells during Dorsal Intercalation

The hypodermis arises as a patch of cells in the posterior of the embryo, and the morphogenetic processes of dorsal intercalation and ventral enclosure occur at approximately the same time on opposite sides of the embryo. During the process of intercalation, the two central rows of cells interdigitate, and their nuclei migrate contralaterally (Sulston *et al.*, 1983). During ventral enclosure, two pairs of cells at the margin of the leading edge initiate migration around the equator of the embryo, and the embryo becomes wrapped in the hypodermal monolayer (Williams-Masson *et al.*, 1997).

It is possible to temporally order dorsal intercalation and ventral enclosure by reconstructing the three-dimensional shape of the embryo from laser-scanning confocal images of wild-type embryos stained with MH27 antibody. The MH27 antibody recognizes a component of the zonulae adherens and can be used to visualize epithelial boundaries during intercalation and ventral enclosure (Francis and Waterston, 1991). Three-dimensional reconstructions of each half of the embryo reveal that before intercalation the hypodermal cells form a dorsal monolayer that wraps slightly around the posterior end of the embryo (Figs. 1A and 1B, arrow). The cells become organized into six rows at the onset of intercalation and change from a rounded shape into a "wedged" shape, with their medial points inserted between their contralateral neighbors (Fig. 1C, arrows). All the cells do not intercalate at the same time; rather, intercalation proceeds from the anterior-most end of the sheet in the posterior direction, with the exception of two pairs of cells (Fig. 1C, arrowheads). These two pairs of cells, which we term "pointer cells," form a wedged shape and remain stationary with their tips touching (Fig. 1C, arrowheads). The other intercalating cells extend their protruding tips between their contralateral neighbors and stretch toward the boundary between the dorsal and lateral cells (Fig. 1E, arrow).

The leading edge of the hypodermis can be seen as it starts to migrate around the periphery of the embryo in a lateral view (Fig. 1F, arrow). The remaining two pointer pairs of dorsal cells intercalate as the hypodermis is enclosing (Fig. 1E, arrowheads), and can be seen just completing intercalation as the ventral cells meet at the midline (Fig. 1G, arrowheads). Thus, dorsal intercalation occurs primarily before the onset of enclosure, but is not complete until after ventral enclosure is well underway.

Dynamic Patterns of Intercalation in Living Embryos

Dorsal intercalation can also be analyzed in living embryos using Nomarski microscopy. In hypodermal tissue visualized by Nomarski microscopy, cellular boundaries appear as depressions in the hypodermal sheet, and nuclei can be visualized as exclusions of cytoplasmic granules (Fig. 2). Playback of time-lapse images allows visualization of the dynamic changes that dorsal cells undergo during intercalation, and concomitant nuclear migration can now be viewed as well. When the cells have mostly intercalated and their tips have almost reached the boundary between the dorsal and lateral cells, the nuclei begin moving toward the tips (Fig. 2A, tips indicated by black arrows). The average nuclear migration rate was calculated to be 11.3 $\pm$ 0.5 μm/h (n = 8 nuclei; mean $\pm$ SD); nuclei migrated at a constant rate once migration was initiated (data not shown).

Differences in dorsal intercalation patterning can also be seen in intercalating cells derived from different lineages. Cells 1–10 are descended from the AB founder cell, whereas the more posterior dorsal cells are derived from the C founder cell. The C-derived cells wedge and intercalate in an anterior-posterior sequence. In contrast, two pairs of AB-derived cells exhibit the "pointing behavior," and the rest of the AB-derived dorsal cells intercalate, but are not originally elongated as much in the mediolateral dimension as the C-derived cells (Fig. 2B, white arrows). The cells in Fig. 2 are numbered corresponding to the designations assigned in Sulston *et al.* (1983). However, it should be noted that on many occasions there was variability in the region of cells 9–11, i.e., cell 10 often migrated anterior to cell 9. Therefore, intercalation is not an entirely invariant process under the conditions used in this study.

Intercalating Cells Undergo Changes in Shape and Surface Area during Intercalation

It is apparent from Nomarski and immunofluorescence microscopy that dorsal hypodermal cells elongate mediolaterally from a rounded shape at the beginning of intercalation to an oblong shape at the end of the process. To better visualize changes in cell shape, we utilized scanning electron microscopy to examine embryos during intercalation. Figure 3A shows an embryo that is nearing the end of the intercalation process. The cells that have completed intercalation and are beginning to stretch mediolaterally are rectangular in shape and are almost the same width along the anterior-posterior axis at their mediolateral ends (Fig. 3A, thin arrows). A few of these cells are still narrower at their migrating ends (arrowheads). The more posterior cells have just completed intercalation and have not yet stretched as far mediolaterally (Figs. 3A and 3C, thick

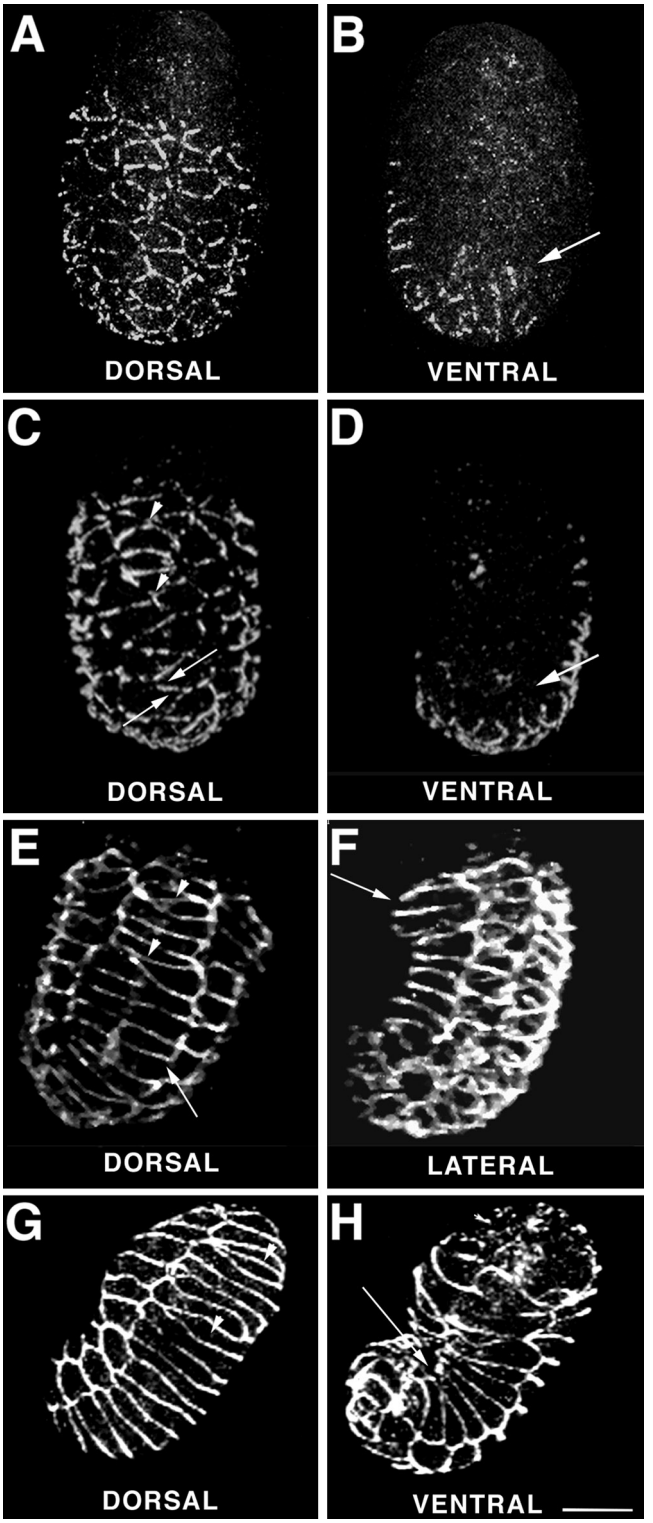

FIG. 1. Three-dimensional reconstructions of MH27 antibody-stained wild-type embryos. The major stages of dorsal intercalation and enclosure are shown sequentially. A, C, E, and G are dorsal views. B, D, and H are ventral views and F is a lateral view of the corresponding embryos in the left-hand column. (A) The hypodermal cell arrangement before intercalation. (B) The hypodermis is wrapped around the posterior onto the ventral side (arrow). C) The hypodermal cells have organized into six rows, and the two innermost rows of cells have begun to intercalate. The "wedged" shape of the intercalating cells is evident (arrows). Two pairs of cells "point" at each other and are last to begin intercalating (arrowheads). (D) Little ventral migration is evident; a small posterior patch of hypodermis is still visible (arrow). (E) All the cells have intercalated and reached the dorsolateral boundary (arrow) except for the "pointer cells" (arrowheads). (F) Lateral view showing the initiation of ventral enclosure by the "leading" cells around the equator of the embryo (arrow). (G) Intercalation is almost complete, including the pointer cells (arrowheads). (H) Ventral enclosure is complete except for a small pocket at the ventral midline (arrow). The anterior is still unenclosed (arrowhead). Anterior is toward the top in all views. Bar, 10 μm.

arrows). These cells are visibly thicker along the dorsoventral axis than their thinned anterior neighbors (Fig. 3C, arrows). The anteriormost hypodermal cells are still actively intercalating and are thinner at the actively intercalating end of the cell (Fig. 3B, arrows). What appears to be a thin protruding tip can be seen extending from one of the intercalating cells between its two contralateral neighbors, and apparently descends toward the basal surface of the two neighboring cells (Fig. 3B, arrowhead). There is a visible difference at the border between the dorsal cells that will fuse and form the *hyp-7* syncytium and the dorsal cells that will fuse and form the *hyp-6* syncytium (Fig. 3A). The future *hyp-7* cells are raised higher in the dorsoventral dimension, and cell 6 at the anterior edge of *hyp-7* (marked with *) is very broad, contrasting with the *hyp-6* cells anterior to it.

Intercalating Dorsal Cells Extend Basal Protrusions Which Precede Junctional Rearrangement

Transmission electron microscopy (TEM) imaging of serial sagittal sections allows detailed examination of an intercalating dorsal cell as it extends between its contralateral neighbors. Figures 4A and 4B show a lateral view in which the dorsal ridge is at the top of the embryo, and the epithelial monolayer is viewed in sagittal section. The apical surface of the monolayer is toward the top and anterior is toward the right in all images. The tip of the intercalating cell (cell 10) is coming out of the plane of the image, emerging between its two contralateral neighbors (Figs. 4A and 4B, black arrow). The initial sections reveal the tip of the intercalating cell (Fig. 4A, arrow); in deeper sections (i.e., sections taken further toward the left side of the embryo), the intercalating cell can be seen to broaden toward its stationary side, which resides at the left dorsolateral boundary (Fig. 4B, arrow).

TEM images were also obtained at higher magnification (Figs. 4C–4F). At the beginning of the series, there are

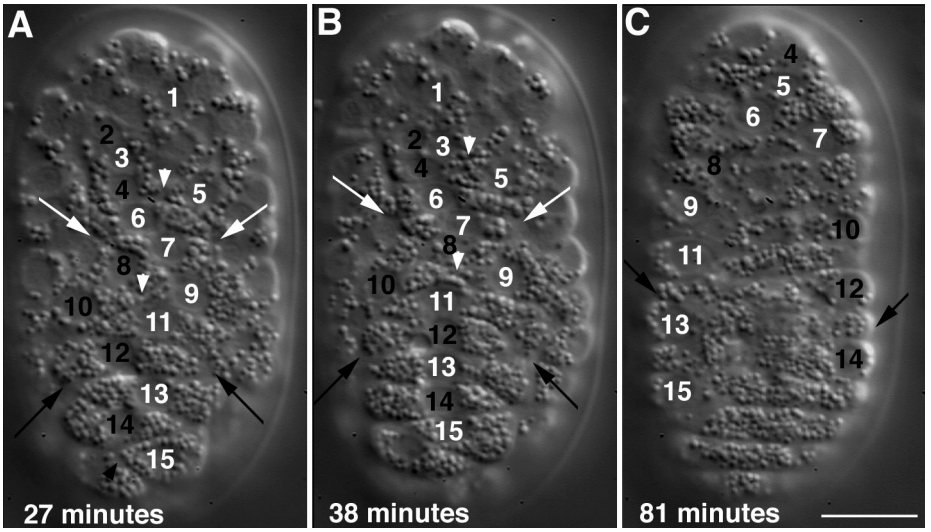

FIG. 2. Nomarski time-lapse videomicroscopy images of wild-type embryos during dorsal intercalation. Cells are numbered according to the convention in Sulston *et al.* (1983). The tips of the two pairs of pointer cells are indicated with white arrowheads (A, B). (A) The more anterior dorsal hypodermal cells have already intercalated and reached the dorsolateral boundary (white arrows). The more posterior dorsal cell tips (11–14) have almost reached the dorsolateral boundaries (black arrows), and the nuclei have begun to migrate. The most posterior cell (15) is wedging and inserting its tip between its contralateral neighbors (black arrowhead). $T = 27$ min. (B) The dorsal cells are completely intercalated and touch the dorsolateral boundaries (black and white arrows), and the nuclei are aligned at the dorsal midline. The pointer cells (4 and 5; 9 and 10) are not yet intercalated, but one pair (4 and 5) are beginning to overlap (arrowheads). $T = 38$ min. (C) The nuclei migrate past the dorsal midline and approach the dorsolateral boundaries (arrows) and the pointer cells have intercalated (4, 5 and 9, 10). $T = 81$ min. Anterior is toward the top and all views are dorsal. Bar, 10 μm.

cellular junctions apical to the intercalating tip (Figs. 4C, 4D, black arrow; Fig. 4C inset, arrowheads). A higher magnification of the intercalating tip (Fig. 4C, inset, arrow) shows that in addition to the junction visible above the tip (black arrowhead), there is also a junctional remnant at the site of insertion of the intercalating cell tip (white arrowhead). In deeper sections, the apical junctions appear broken (Fig. 4E, black arrow). The leftmost sections cut through the side of the cell touching the dorsolateral boundary, where the cell is almost as broad as its neighbors, and close membrane appositions are apparent between the intercalating cell and its anterior and posterior neighbors (Fig. 4F).

A three-dimensional reconstruction of the tip of the intercalating cell was made using the first 24 sections of the cell, corresponding to ≈ 2 μm. (Fig. 4G). The zonulae adherens are shown in gray, and the intercalating cell in red. An apical view of the reconstruction shows the intercalating cell extending a tip (arrow) between its contralateral neighboring cells (the cell bodies are not shown in the reconstruction). The zonula adherens (arrowhead) is visible apical to the protruding tip. A lateral view of the same intercalating tip shows the zonula adherens (arrowhead) connecting the contralateral cells suspended above the basal tip (arrow). For clarity, the two neighboring cells are not shown in the reconstruction; hence, the junction is suspended above the intercalating cellular protrusion. The arrowhead marks the junctional position which we believe corresponds to the tip of the wedging cells visualized by MH27 antibody staining (see Fig. 1C, arrows). The zonula adherens is much thinner at this point of contact between the wedging cell and its two contralateral neighbors, presumably because the basal protrusion of the intercalating tip is breaking down the zonulae adherens as the cell moves forward.

Thus, as a dorsal cell migrates between its neighbors, it inserts a basal protrusion underneath the zonulae adherens of two opposing cells. As the cell migrates, it becomes broader in the apical–basal and anterior–posterior dimensions, and effectively "plows" through the contralateral cells, apparently breaking open their apical junctional connections as it pushes underneath and between the two opposing cells.

Anterior Hypodermal Cells Intercalate in the Absence of the Posterior Hypodermis

Ablation of the nucleus of the C founder cell at the 10-cell stage results in an embryo lacking posterior hypodermis, as well as some neuronal and muscle tissue. The C founder cell was ablated in 15 embryos and the embryos were assayed for intercalation via Nomarski microscopy. In all cases, the AB-derived cells intercalated in the absence of any posterior hypodermis (Fig. 5A, white arrows and arrowheads). The ablated C cell is visible as a large cell near the midline at the posterior of the embryo (Fig. 5A, black

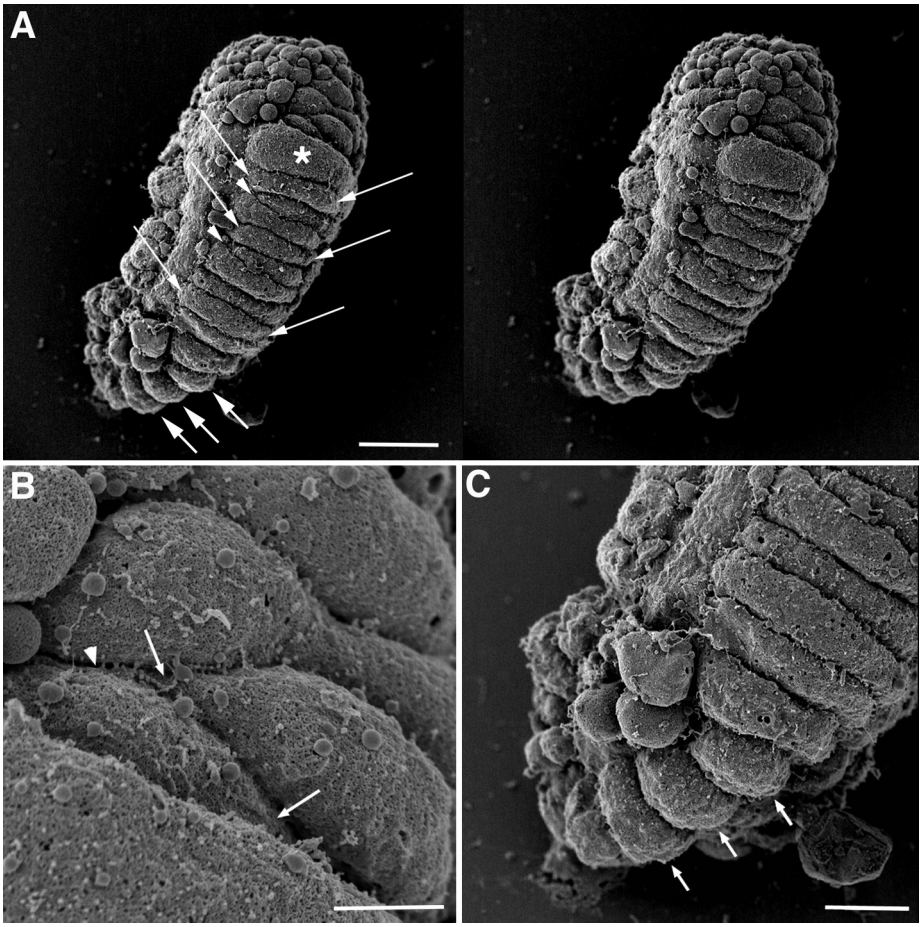

FIG. 3. Scanning electron micrographs of an embryo that is undergoing the late stages of intercalation. (A) Most of the more anterior dorsal cells have completed intercalation and are the same width along the anterior-posterior axis (arrows). A few cells have not yet completely intercalated, and their more narrow tips are evident (arrowheads). The more posterior dorsal cells are just finishing intercalation, and are not yet as stretched in the mediolateral direction (short arrows). (B) The anterior pair of pointer cells, 4 and 5, are in the process of intercalating (arrows). The cells can be seen to extend long protrusions in the direction of migration, which appear to extend downward (i.e., basally) between the neighboring cells (arrowhead). (C) The more posterior cells are still somewhat rounded, are not stretched as much mediolaterally, and are visibly thicker in the dorsoventral plane (arrows). All views are dorsal, with anterior toward the top. Bar, 10, 2, and 4 μm, respectively.

arrow). The ablated embryos always turned ventrally during subsequent development but intercalation could be readily followed by focusing through the embryo.

Hypodermal Cells Intercalate in the Absence of Half of the Lateral Hypodermis

The lateral hypodermal cells form a row of 10 cells on each side of the dorsal cells and could provide a signal to guide dorsal cells during intercalation, or provide a signal to intercalating cells to cease rearranging. To assess the role of lateral cells during intercalation, laser ablation of the nucleus of the progenitor cell for half of the lateral hypodermis, ABarpp, was performed. The ABarpp cell gives rise to 12 hypodermal cells; 10 lateral cells, 5 on each side of the animal, and 2 dorsal cells. The 10 lateral cells are termed H2L/R, V1L/R, V2L/R, V4L/R and V6L/R, and the two dorsal cells are ABarpppapa and ABarppaapa, corresponding to cells 9 and 10 in Fig. 2 (Sulston *et al.*, 1983).

Embryos of a strain of *C. elegans* that carries a seam cell-specific green fluorescent protein transcriptional reporter (Terns *et al.*, 1997; Gendreau *et al.*, 1994) were collected and mounted as 2-cell embryos, and the nucleus of ABarpp was ablated approximately 10 min after division of ABarp. Ten embryos were ablated, and all 10 embryos enclosed and elongated, with the exception of one embryo that died during elongation (Figs. 5B and 5C). The intercalation process was recorded by 4D time-lapse microscopy in the embryos whose dorsal hypodermis was toward the coverslip (n = 3). Ablation of the ABarpp cell

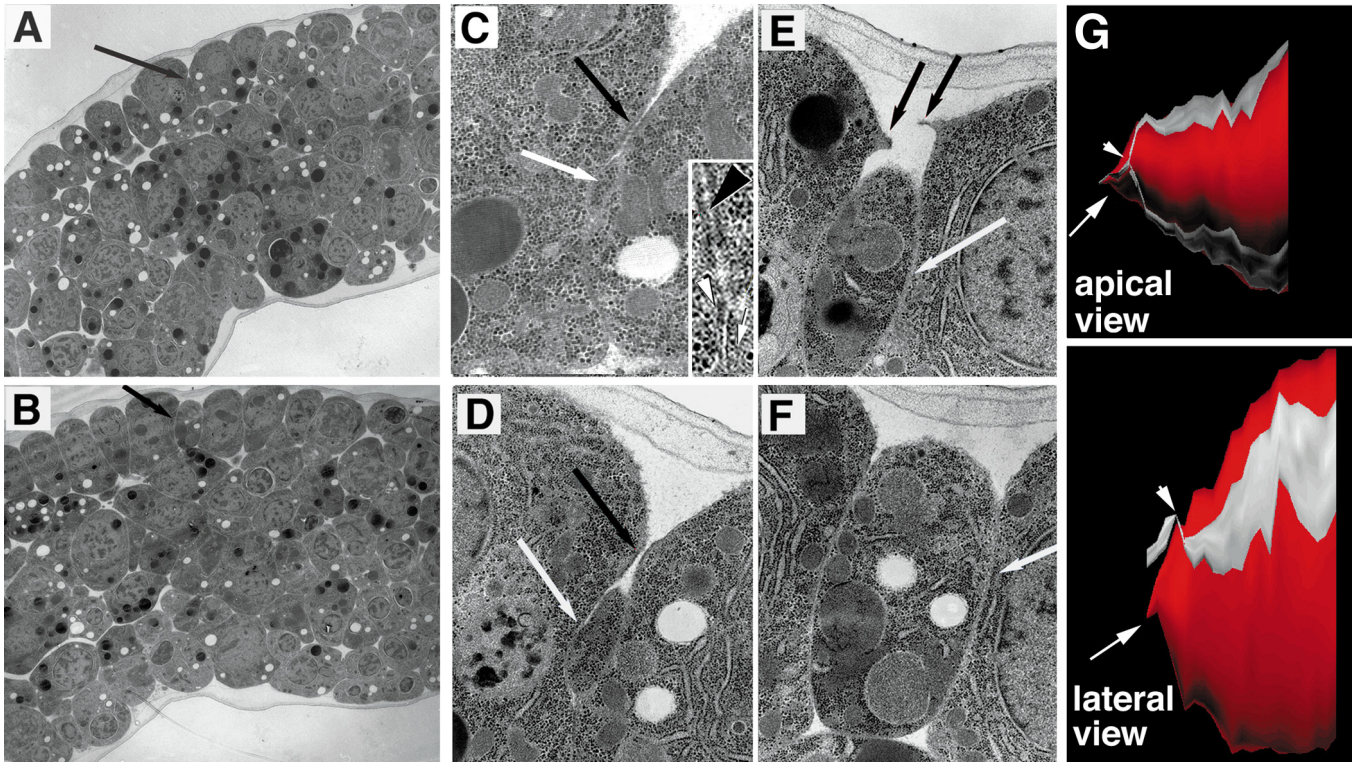

FIG. 4. Transmission electron microscopy (TEM) of intercalating dorsal cells shown in a lateral view of a wild-type embryo. (A, B) The tip of a cell (arrow) that is intercalating between its two neighboring cells is moving out of the plane of the image toward the viewer. The arrow marks the intercalating tip as it enlarges in the deeper section. Original magnification, 2800×. (C–F) The same intercalating cells (in a series of more closely spaced sections) shown at higher magnification (24,000×). The white arrows show the general location of the intercalating tip. The black arrows show the location of what is believed to be the zonulae adherens (C, D) or its remnants (E). A magnification of the intercalating tip (C, inset) shows the protrusion of the intercalating cell (white arrow) beneath the zonulae adherens (black arrowhead). The white arrowhead points to what appears to be remnants of the zonulae adherens that have been broken by the advancing tip. (G) A three-dimensional reconstruction of the tip of the intercalating cell shown in A–F. The adherens junctions between the intercalating cell and its contralateral neighbors (not shown in the reconstruction) are shown in gray; the intercalating cell is shown in red. The intercalating cell extends a basal protrusion (arrow) that is inserted beneath the adherens junction (arrowhead). All views in A–F are lateral, anterior to the right.

results in the loss of the posteriormost two cells of the AB-derived hypodermis, so when the dorsal cells in an ablated embryo begin to intercalate, there is a cleft between the dorsal cells of the AB lineage (Fig. 5B, black arrow) and those of the C lineage (Fig. 5B, white arrow). The two populations of cells wedge and intercalate normally, and at the end of intercalation are pulled into a contiguous row of cells as the embryo encloses (Fig. 5B; data not shown). Nine of the 10 ablated animals enclose, elongate, and hatch, although their development is slowed (Fig. 5C). Scoring of the GFP seam cell marker showed that 5 lateral cells were missing on each side of the animal ($n = 9$) (Fig. 5D). Thus, embryos which lack half of their lateral hypodermis are able to intercalate and develop normally, even though the line of cells which normally delineate the zone of intercalation have been depleted.

Microtubules Begin Aligning Circumferentially during Intercalation

Changes in the cytoskeleton usually accompany the movement of cells. To examine microtubule structure in intercalating cells, embryos were fixed and stained with the *mcap 77* antibody, which recognizes α-tubulin. At the beginning of intercalation, the wedging cells exhibit a meshwork of microtubules that reside in a thin layer (Fig. 6A). By the time the cells have intercalated, some circumferential alignment of microtubules can be observed (Fig. 6B). There is a heavy localization of microtubules parallel to the mediolateral cell boundaries (Fig. 6B, arrows). The nuclei are visible as black regions that exclude microtubules (Fig. 6B, arrowheads). Approximately 30 min later, when enclosure is complete, further alignment of microtubules is apparent (Fig. 6C).

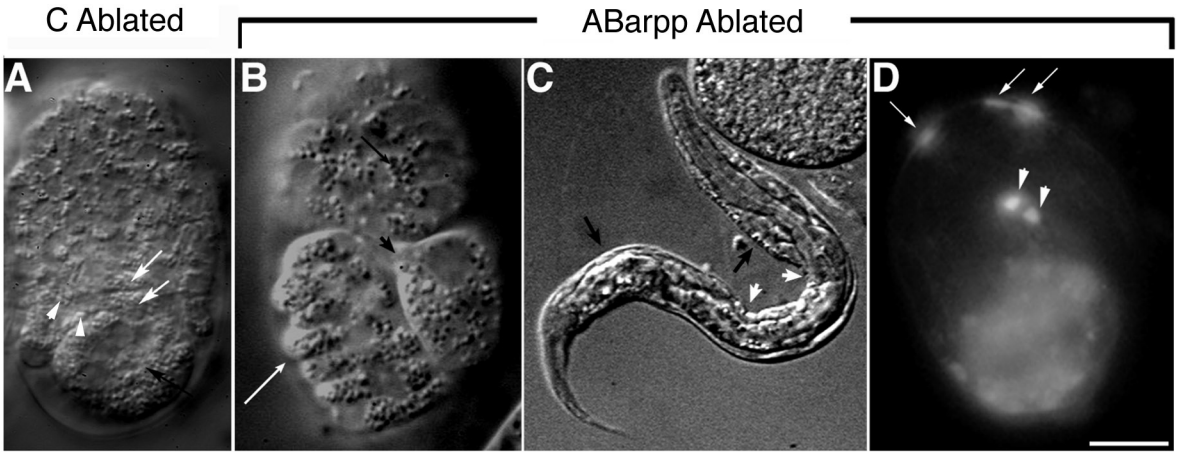

FIG. 5. Ablation of progenitors of hypodermal cells adjacent to intercalating cells. (A) The nucleus of the C founder cell was ablated at the 10-cell stage and intercalation and enclosure were followed. Anterior hypodermal cells (white arrows and arrowheads) are AB descendants, and are beginning to wedge and intercalate in the absence of posterior hypodermal cells, which are C-derived. The ablated C cell remnant is visible at the posterior (black arrow). (B) The nucleus of the ABarpp cell was ablated approximately 10 min after the division of ABarp. The cells derived from the AB progenitor cell (black arrows) were separated from the cells derived from the C progenitor cells (white arrows) by the carcass of the dead ABarpp remnant (arrowhead). The two populations of cells (arrows) intercalate normally, and the carcass (arrowhead) is squeezed out as the two populations are pulled into a straight line during enclosure. (C) The embryo encloses and elongates. Localized constrictions (white arrows) and bulges (black arrows) are presumably due to the regional absence of hypodermal tissue. (D) The expression of the GFP seam cell marker shows that only 5 of the 10 seam cells are present (arrows and arrowheads), with the appropriate cell gap between HO, H1 and V3 (arrows). Anterior is up in all views. A and B are dorsal views. Bar, 10 μm.

Actin Microfilaments Align Circumferentially after Intercalation

Embryos were fixed and stained with phalloidin and viewed via confocal microscopy. At the onset of intercalation, the microfilaments are arranged in a meshwork on the apical surface of the cells, much as the microtubules are (Fig. 7A). By the end of intercalation, the actin microfilaments are still organized as a meshwork (Fig. 7B), but begin to align circumferentially near the end of ventral enclosure in preparation for elongation (Fig. 7C).

Both Microtubules and Microfilaments Are Necessary for Cell Rearrangement

To examine requirements for cytoplasmic microtubules during intercalation, embryos were mounted in embryonic growth medium + 1 μg/ml nocodazole and laser permeabilized at the beginning of dorsal intercalation. Successful permeabilization was indicated by the presence of blue gut granules 3–4 h after permeabilization, caused by the presence of Nile blue A in the medium. Five embryos were analyzed during dorsal intercalation. In all five experiments, nuclear migration was completely halted (Fig. 8B), and the embryos failed to elongate.

The embryos were laser permeabilized as the posterior cells were wedging and beginning to extend their tips toward the opposing dorsolateral boundary. At this stage, the pointer cells have not yet started intercalating. In all cases, the wedging cells continue migrating at first, to varying degrees. However, the cells stop migrating before or as the nuclei cease migrating. Figure 8B shows such an embryo. The cells extended further toward the boundary after permeabilization, but many did not reach the boundary before halting. Significantly, the "pointer" cells did not intercalate in these embryos (Fig. 8B, arrows). The subsequent cessation of cellular movement in the pointer cells shows that nocodazole can specifically block intercalation of identified dorsal hypodermal cells following their exposure to the drug.

To examine requirements for actin microfilaments during intercalation, embryos were mounted in EGM + 2 μg/ml cytochalasin D and laser permeabilized during dorsal intercalation. The most immediate and obvious effect of cytochalasin D was to cause all epithelial boundaries to become indistinct, making the analysis of cell rearrangement difficult. However, several conclusions can be drawn from the data. Two embryos were permeabilized early in intercalation, and both of these embryos ceased intercalating almost immediately. Dorsal hypodermal cells that had started to wedge when the embryos were permeabilized continued wedging briefly before ceasing to intercalate (Fig. 8C, white arrows). Three embryos were permeabilized when intercalation was already underway, and in all three experiments, the pointer cells did not intercalate and the nuclei either slowed or stopped migrating (data not shown). Thus, cytochalasin D stops cell rearrangement during dorsal intercalation, and can halt nuclear migration as well.

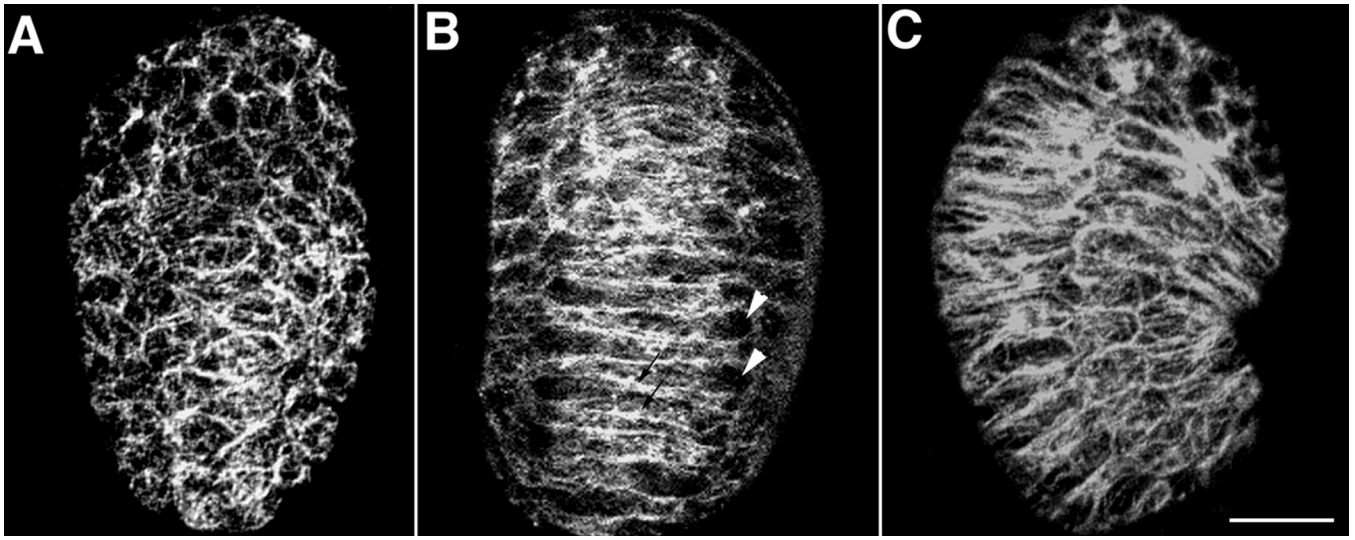

FIG. 6. Microtubule distribution during dorsal intercalation. (A) The microtubules are arranged in a meshwork at the beginning of intercalation as the cells are wedging. (B) The microtubules start to become circumferentially aligned by the time the cells have intercalated. There is a heavy localization of microtubules along cellular boundaries, and thick strands of microtubules are visible parallel to the boundaries (arrows). The nuclei are visible as areas that exclude microtubules (arrowheads). (C) Further alignment of microtubules is apparent when enclosure is complete. A and B are dorsal views, and C is a lateral view. Bar, 10 μm.

DISCUSSION

A Model for Rearranging Epithelial Cells: Basal Protrusions Extend beneath the Zonulae Adherens of Intercalating Cells

Understanding the behavior of rearranging cells is a central problem in morphogenesis, yet analysis of patterns of cell rearrangements is often difficult. The largely invariant process of hypodermal morphogenesis in the nematode *C. elegans* provides an excellent model for elucidating the cellular and molecular mechanisms of epithelial cell rearrangement. Our results represent the first detailed characterization of epithelial cells that are known to be in the process of rearrangement.

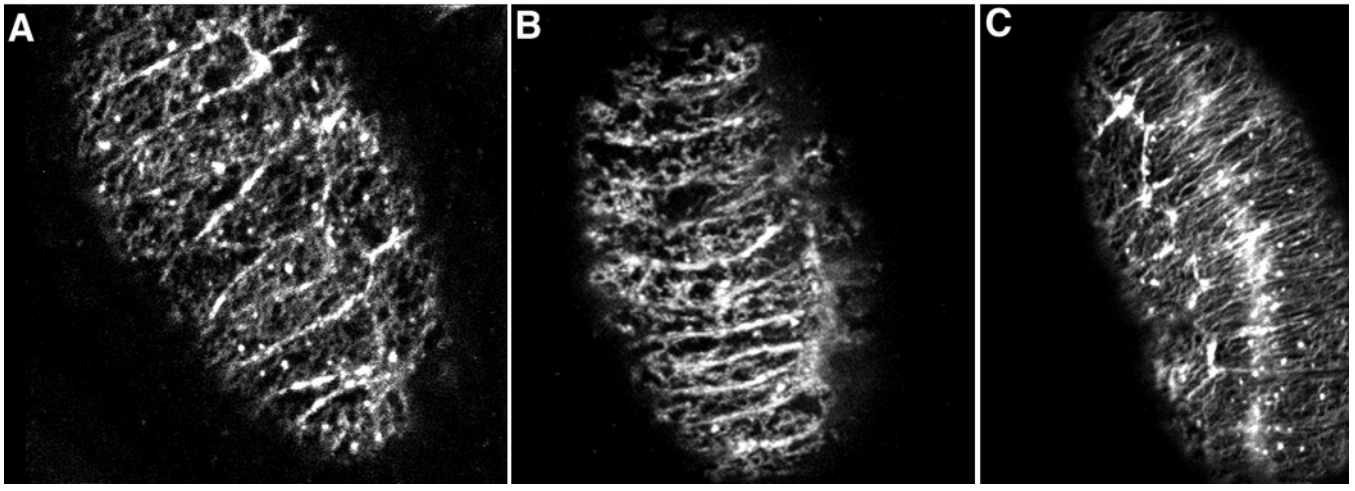

FIG. 7. Actin microfilament distribution during dorsal intercalation. (A, B) Dorsal views of embryos that are wedging (A) and completing intercalation (B). The actin meshwork is apical to the zonulae adherens and not yet strongly aligned circumferentially. (C) Dorsal view of an embryo that has completed intercalation and is mostly enclosed. The actin microfilaments are no longer organized randomly, and show a strong bias toward circumferential alignment. Bar, 10 μm.

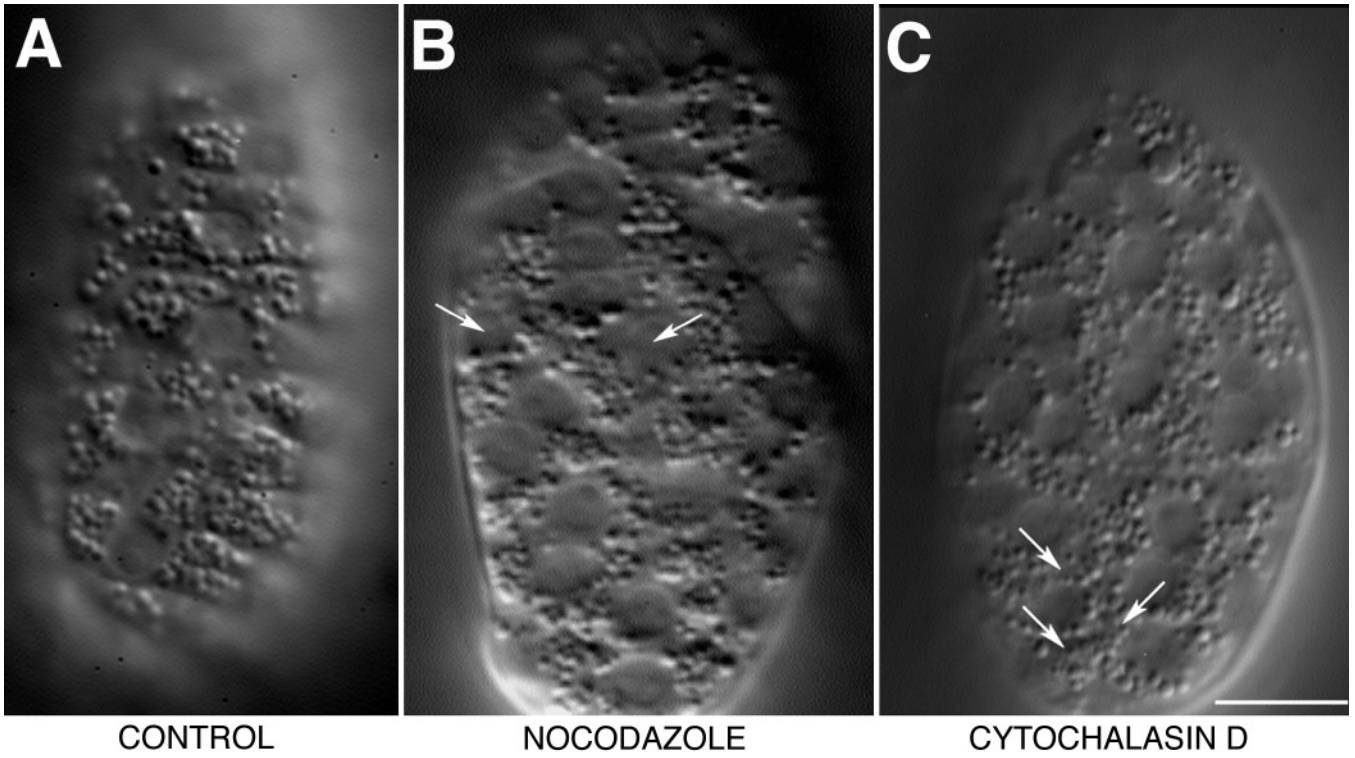

FIG. 8. Disruption of microtubules and microfilaments during dorsal intercalation. Wild-type embryos were mounted in embryonic growth medium + 1 μg/ml nocodazole (B) or 2 μg/ml cytochalasin D (C) and laser permeabilized at the beginning of intercalation. (A) A wild-type embryo at a comparable time in development to the drug-treated embryos. The dorsal cells have completely intercalated. (B) An embryo that was permeabilized in nocodazole when the cells were partially intercalated. The cells continue migrating for a few minutes, but some do not reach the dorsolateral boundary before ceasing migration. Notably, the pointer cells fail to intercalate (arrows), and the nuclei do not migrate. (C) An embryo that was permeabilized in cytochalasin D as the dorsal cells began to wedge. The dorsal cells continue wedging briefly and then stop migrating. Arrows show the tips of the wedging cells. The dorsal nuclei never migrate. All views are dorsal, anterior is to the top. Bar, 10 μm.

We propose a model for how hypodermal cells can rearrange within the confines of an epithelial sheet while maintaining epithelial integrity (Fig. 9). SEM and TEM images reveal the presence of a thin protrusion at the tip of an intercalating cell. Serial sagittal sections reveal that this protrusion is basolateral, and appears to wedge itself under the zonulae adherens, along the boundary between the two contralateral neighbors of the intercalating cell. The intercalating cell pushes forward toward the dorsolateral boundary, and the widening basal tip effectively plows through the zonulae adherens. As the cell migrates forward, apical membrane is apparently inserted at the site of intercalation, thereby creating a new junction-bounded domain between the two opposing cells. The intercalating cell forms junctions with its new neighbors, thus preserving epithelial integrity. This is the first demonstration at the ultrastructural level of how epithelial cell rearrangement is accomplished. This analysis is enabled by the reproducibility of cell rearrangement in this system, allowing individual cells of known identity to be analyzed.

Simultaneous visualization of the plasma membrane with a vital membrane dye and adherens junctions using a MH27-GFP translational fusion confirms the existence of the basal protrusions (B. Mohler and J. Simske, personal communication). The nuclei in these dorsal cells were also visible moving beneath the adherens junctions and into the basal tips. Based upon these observations using double staining in living embryos, it would appear that the intercalation patterns seen in conventional MH27 antibody staining temporally lag behind the events seen in Nomarski microscopy, since the Nomarski images are actually showing the activities of the basal tips, as evidenced by the presence of the migrating nuclei. These basal tips reach the dorsolateral boundaries before any changes are seen at the level of the adherens junctions, supporting our conclusion that it is the widening base of the basal tip that forms new junctions with its neighboring cells after the basal protrusion has extended beneath and through the zonulae adherens.

An Intact Cytoskeleton Is Necessary for Initiation of Intercalation

Exposure of embryos to the drugs nocodazole and cytochalasin D affected both nuclear migration and cell rear-

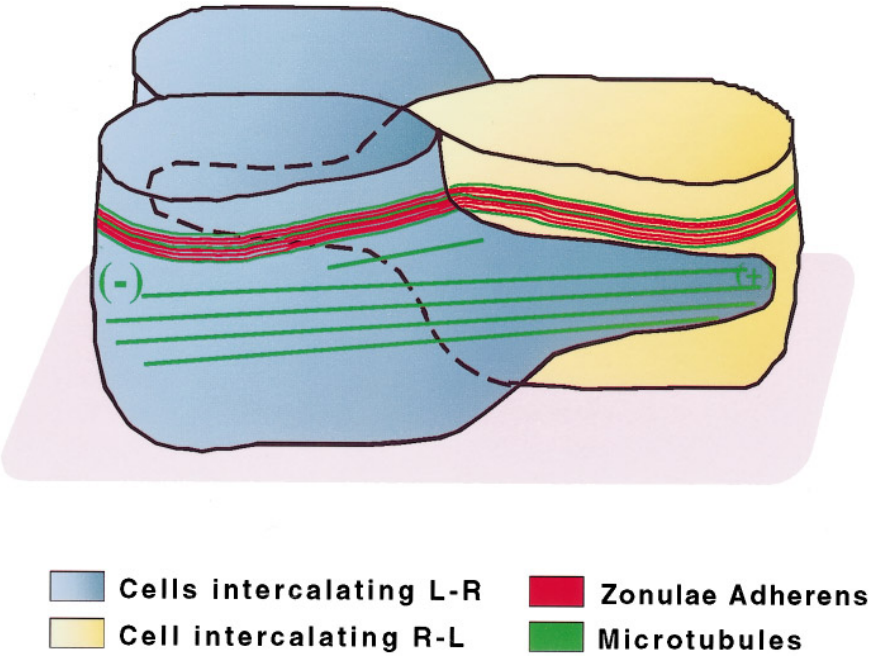

FIG. 9. A schematic diagram illustrating the mechanism of dorsal cell intercalation based upon a compilation of transmission and scanning electron microscopy, Nomarski microscopy and antibody staining with MH27 (which recognizes a component of the zonulae adherens, in red) and *mcap-77* (which recognizes α- tubulin, in green). The two blue cells are intercalating from the left side toward the right side of the embryo, and the yellow cell is intercalating from the right side toward the left. All the cells extend a basal protrusion toward the dorsolateral boundary that may be strengthened with an array of microtubules (green). During intercalation, rearranging cells migrate along a substratum that is in contact with their basal surfaces (either extracellular matrix or underlying cells, shown in pink).

rangement. The disruptive effects seen during the drug experiments were not merely due to embryonic death, since the embryos usually began twitching at a later time, consistent with normal muscle development. It is possible that the cells stopped rearranging because the drugs were interfering with ventral enclosure, as we have shown in the case of cytochalasin D (Williams-Masson *et al.*, 1997); however, dorsal intercalation is primarily completed before the initiation of ventral enclosure, so it is unlikely that epiboly is driving the intercalation of most of the dorsal cells.

That nocodazole would block nuclear migration is not surprising, given that nuclear migration is also blocked by mutations in the *unc-116* kinesin heavy chain, a microtubule motor protein (Patel *et al.*, 1993). The fact that cytochalasin D slowed nuclear migration is somewhat surprising; however, the collapse of the actin cytoskeleton is so dramatic in these experiments that it is possible that microtubule organization is also perturbed once the cell cortex and apical microfilaments are destabilized. Nuclear migration is never completely blocked in embryos by cytochalasin D treatment unless cell rearrangement is also blocked, and we have shown that nuclear migration does not begin until cell rearrangement is largely complete, and the cellular tips have almost reached the dorsolateral boundaries.

In most cases in which a cell was exposed to either drug before it began changing shape, the cell was unable to subsequently migrate. This was clear in the case of the "pointer" cells which were blocked from migrating by drug treatment, and all the cells could be blocked if exposed to the drugs at an early stage. Thus, it is probable that both intact microfilaments and microtubules are required for the necessary shape changes concomitant with cellular migration.

At first glance, it is somewhat surprising that microtubules would be required for cell rearrangement. However, Lane and Keller (1997) have shown that microtubules are necessary for orienting and polarizing the first deep, nonepithelial cells that undergo mediolateral intercalation during *Xenopus* gastrulation, but that subsequent intercalating cells are able to intercalate in the absence of microtubules. They suggest that microtubules are necessary for cell polarization by stabilizing filopodia at the medial and lateral ends of the cells, and that the second population of intercalating cells that are microtubule-independent become entrained by the lead of the initial intercalating cells.

The dorsal cells of the *C. elegans* hypodermis appear dependent upon the presence of microtubules to begin intercalating. Microtubules are thought to provide rigidity in a tissue (Joshi *et al.*, 1985), and it is possible that the

wedging tips need to be rigid to force their way between neighboring contralateral cells. If this were the case, cells that have been exposed to nocodazole would lose rigidity and be unable to extend between their contralateral neighbors.

Cytochalasin D blocks dorsal intercalation; yet, we have not been able to visualize any specific actin microfilament organization in the intercalating tips, in contrast to the protrusions that are apparent in the "leading cells" that migrate around the periphery of the embryo during enclosure (Williams-Masson *et al.,* 1997). The effects of cytochalasin D may be on the cortex and structural cytoarchitecture of the cell, rather than specific structures required for dorsal intercalation. Alternatively, the actin-requiring structures affected may be beyond the resolution of the techniques we have employed in this study.

Embryos that were exposed to either nocodazole or cytochalasin D also failed to undergo ventral enclosure and elongation. This failure in subsequent morphogenetic processes is not necessarily caused by a lack of dorsal intercalation, however. We have previously shown that cytochalasin D blocks ventral enclosure (Williams-Masson *et al.*, 1997), and Priess and Hirsh (1986) have shown that either cytochalasin D or nocodazole treatment of elongating embryos blocks elongation. Therefore, an intact actin and/or microtubule cytoskeleton is essential for ventral enclosure and elongation, and the failure of the embryos to elongate in the experiments described in this study does not directly address whether dorsal intercalation is necessary for ventral enclosure and elongation.

Dorsal Cells Do Not Appear to Require Neighboring Hypodermal Cells to Intercalate

Absence of the posterior hypodermis does not prevent intercalation of the anterior hypodermal cells, suggesting that long-range anterior–posterior signaling from the dorsal hypodermis is not responsible for the initiation of dorsal intercalation. Likewise, ablation of the progenitor cell for half of the lateral cells does not block dorsal intercalation, indicating that the normal, local interactions between specific lateral and dorsal cells are not required for intercalation. Preliminary experiments involving laser ablations of neighboring dorsal cells show no interference of an individual dorsal cell's ability to intercalate, suggesting that the primary cue for dorsal intercalation may reside in the migrating cells' substratum or underlying cells (E. Williams-Masson, unpublished observations).

Directional cues could be produced by the lateral cells or the underlying muscle cells or they might reside in the extracellular matrix. Ablation of the progenitor cell for half of the lateral cells does not disrupt dorsal intercalation, suggesting that a signal emanating from the lateral cells is not responsible for directed cell migration unless the remaining lateral cells in the ABarpp ablation experiment are able to produce sufficient amounts of signal. At present, it appears more likely that either the muscle cells produce such cues or that the dorsal cells are responding to a cue within the basement membrane.

Alternatively, it is possible that the dorsal cells are undergoing sorting based upon differences in cell adhesion or some other membrane component. Tepass *et al.* (1996) have shown that zygotic Shotgun protein, the *Drosophila* E-cadherin homolog, is required for cell rearrangement in Malpighian tubule precursors. Recently, genes involved in cadherin-based adhesion have been characterized in *C. elegans,* but no major defects have been reported in dorsal intercalation when these components are mutated (Costa *et al.*, 1998). Furthermore, since dorsal cells appear to migrate independently of their normal neighboring dorsal hypodermal cells, it seems more likely that directional cues in the substratum play a more pivotal role in dorsal intercalation.

Nuclear Migration Is Functionally Irrelevant for Dorsal Intercalation

Contralateral nuclear migration begins in the dorsal cells after the cells have largely completed intercalation, as we have shown in wild-type embryos. The absence of nuclear migration does not affect cell rearrangement or ventral enclosure, as evidenced by the completion of these processes in *unc-83 (e1408)* embryos, which intercalate and enclose normally in the absence of complete nuclear migration (Sulston *et al.,* 1983; E. Williams-Masson, unpublished observations). In wild-type embryos, the cytoskeleton becomes organized parallel to the cellular boundaries of the dorsal cells after they have extended mediolaterally. Nuclear migration would be initiated by the alignment of microtubules if the microtubules shared the same polarity and if the nuclei were associated with a microtubule motor protein. The gene *unc-116* has been shown to encode the heavy chain of a kinesin-related protein, and weak loss of function mutations in this gene results in nuclear migration failure. Kinesins are typically plus-end-directed microtubule motor proteins. If the microtubule organizing centers were located at the stationary base of the cells and the microtubules consequently elongate their plus ends toward the tips of the intercalating cells, the nuclei would migrate toward the cell tips when sufficient microtubules had become polarized (Fig. 9). The data support this model, in that each cell's nucleus migrates toward its own tip, resulting in the alternating nuclear migration pattern seen.

What Does Dorsal Intercalation Accomplish?

The organization of cytoskeletal components is crucial for the successful completion of elongation, a major morphogenetic event that occurs immediately after ventral enclosure (Priess and Hirsh, 1986). Dorsal intercalation may allow for alignment of the cytoskeletal network in dorsal hypodermal cells in preparation for elongation, and nuclear migration may simply occur as a consequence of having a large proportion of the microtubules aligned in a polar fashion as the cells complete intercalation. The organiza-

tion of actin microfilament arrays occurs after the organization of the microtubule arrays, since actin is arranged in a meshwork pattern throughout dorsal intercalation and well into ventral enclosure (Fig. 8). It is possible that the role of dorsal intercalation in hypodermal morphogenesis is to align the microtubule framework, which then permits the subsequent circumferential alignment of the actin microfilaments.

Recent analysis of a mutant defective in dorsal intercalation provides corroborative evidence that dorsal intercalation is essential for successful elongation (P. Heid, B. Raich, S. Gendreau, J. Rothman, and J. Hardin, manuscript in preparation). *die-1* mutants arrest as 1.5- to 2-fold embryos, fail to undergo complete dorsal intercalation, and yet undergo hypodermal enclosure and fusion normally. Cloning of *die-1* (*d*orsal *i*ntercalation and *e*longation defective) reveals the gene to encode a zinc finger protein, suggesting that it may function as a transcription factor. Intriguingly, the Bric-a-brac protein, a nuclear protein that may be involved in transcriptional regulation in *Drosophila,* has been shown to be required for cell rearrangement during the formation of terminal filaments in the ovary (Godt and Laski, 1995).

The method by which dorsal cells intercalate may serve as a general model by which epithelial cells can rearrange while simultaneously preserving tissue integrity. Through characterizing the process of dorsal intercalation in wild-type embryos, we have provided the background for a molecular understanding of epithelial cell rearrangement.

ACKNOWLEDGMENTS

We are grateful to J. Priess, L. Edgar, and C. Shelton for technical advice on the laser permeabilization experiments and mounts. We thank H. Ris and Y. Chen for their assistance with the SEM fixation and imaging, and R. Bromberg of the Electron Microscopy Facility at the University of Wisconsin School of Veterinary Medicine for sectioning the embryos. We are also grateful to R. Terns, I. Hope, M. Fukuyama, J. Kasmir, and J. H. Rothman for providing the GFP seam cell marker strain used in the lateral hypodermal studies. We also thank B. Mohler and J. Simske for their personal communication about the GFP/FM4-64 experiments. We thank S. Gendreau and I. Moskowitz for sharing unpublished results of C and ABarpp ablations with us. We also gratefully acknowledge the help and advice of the members of the laboratory of J. Rothman during the early phases of this and other projects. They were instrumental in helping us to begin studying *C. elegans* embryos. We are grateful to P. Masson, B. Mohler, and J. Simske for critical review of the manuscript, and L. Olds and P. Masson for advice on the illustrations. E. M. Williams-Masson was supported in part by funds from NIH Biotechnology Training Grant GM08349. This work was also supported by a Lucille P. Markey Scholar Award in the Biomedical Sciences and a NSF Young Investigator Award to J. Hardin. The Integrated Microscopy Resource at the University of Wisconsin–Madison is funded as an NIH Biomedical Research Technology Resource.

REFERENCES

Condic, M., Fristrom, D., and Fristrom, J. (1991). Apical cell shape changes during *Drosophila* imaginal leg disc elongation: A novel morphogenetic mechanism. *Development.* **111,** 23–33.

Costa, M., Draper, B. W., and Priess, J. R. (1997). The role of actin filaments in patterning the *Caenorhabditis elegans* cuticle. *Dev. Biol* **184,** 373–384.

Costa, M., Raich, W., Agbunag, C., Leung, B, Hardin, J., and Priess, J. R. (1998). A putative catenin–cadherin system mediates morphogenesis of the *Caenorhabditis elegans* embryo. *J. Cell Biol.*, in press.

Ettensohn, C. A. (1985). Gastrulation in the sea urchin embryo is accompanied by the rearrangement of invaginating epithelial cells. *Dev. Biol.* **112,** 383–390.

Francis, R., and Waterston, R. H. (1991). Muscle cell attachment in *Caenorhabditis elegans. J. Cell Biol.* **114,** 465–479.

Fristrom, D. (1976). The mechanism of evagination of imaginal disks of *Drosophila melanogaster.* III. Evidence for cell rearrangement. *Dev. Biol.* **54,** 163–171.

Gendreau, S. B., Moskowitz, I. P., Terns, R. M., and Rothman, J. H. (1994). The potential to differentiate epidermis is unequally distributed in the AB lineage during early embryonic development in *C. elegans. Dev. Biol.* **166,** 770–781.

Godt, D., and Laski, F. A. (1995). Mechanisms of cell rearrangement and cell recruitment in *Drosophila* ovary morphogenesis and the requirement of *bric a brac. Development* **121,** 173–187.

Hardin, J**.** (1989). Local shifts in position and polarized motility drive cell rearrangement during sea urchin gastrulation. *Dev. Biol.* **136,** 430–445.

Hardin, J. D., and Cheng, L. Y. (1986). The mechanisms and mechanics of archenteron elongation during sea urchin gastrulation. *Dev. Biol.* **115,** 490–501.

Hohenberg, H., Mannweiler, K., and Muller, M. (1994). High-pressure freezing of cell suspensions in cellulose capillary tubes. *J. Microsc.* **175,** 34–43.

Irvine, K. D., and Wieschaus, E. (1994). Cell intercalation during *Drosophila* germband extension and its regulation by pair-rule segmentation genes. *Development.* **120,** 827–841.

Joshi, H. C., Chu, D., Buxbaum, R. E., and Heidemann, S. R. (1985). Tension and compression in the cytoskeleton of PC12 neurites. *J. Cell Biol.* **101,** 697–705.

Keller, R. E., and Tibbetts, P. (1989). Mediolateral cell intercalation is a property of the dorsal, axial mesoderm of *Xenopus laevis. Dev. Biol.* **131,** 539–549.

Keller, R. E., and Trinkaus, J. P. (1987). Rearrangement of enveloping layer cells without disruption of the epithelial permeability barrier as a factor in *Fundulus* epiboly. *Dev. Biol.* **120,** 12–24.

Lane, M. C., and Keller, R. (1997). Microtubule disruption reveals that Spemann's organizer is subdivided into two domains by the vegetal alignment zone. *Development* **124,** 895–906.

Malecki, M., and Ris, H. (1992) Surface topography and intracellular organization of human cells in suspension as revealed by scanning electron microscopy. *Scannning* **14,** 76–85.

Patel, N., Thierry-Mieg, D., and Mancillas, J. R. (1993). Cloning by insertional mutagenesis of a cDNA encoding *Caenorhabditis elegans* kinesin heavy chain. *Proc. Natl. Acad. Sci. USA* **90,** 9181–9185.

Podbilewicz, B., and White, J. G. (1994). Cell fusions in the developing epithelia of *C. elegans. Dev. Biol.* **161,** 408–424.

Priess, J. R., and Hirsh, D. I. (1986). *Caenorhabditis elegans* morphogenesis: The role of the cytoskeleton in elongation of the embryo. *Dev. Biol.* **117,** 156–173.

Ris, H. (1985). The cytoplasmic filament system in critical point-dried whole mounts and plastic-embedded sections. *J. Cell Biol.* **100,** 1474–1487.

Ris, H., and Malecki, M. (1993) High resolution field emission scanning electron microscope imaging of internal cell structures after epon extraction from sections: A new approach to correlative ultrastructural and immunocytochemical studies. *J. Struct. Biol.* **111,** 148–157.

Schoenwolf, G. C., and Alvarez, I. S. (1989). Roles of neuroepithelial cell rearrangement and division in shaping of the avian neural plate. *Development.* **106,** 427–439.

Sulston, J. E., and Hodgkin, J. (1988). Methods. *In* "The Nematode *Caenorhabditis elegans*" (W. B. Wood, Ed.), pp. 587–606. Cold Spring Harbor Laboratory Press, Cold Spring Harbor, NY.

Sulston, J. E., Schierenberg, E., White, J. G., and Thomson, J. N. (1983). The embryonic cell lineage of the nematode *Caenorhabditis elegans. Dev. Biol.* **100,** 64–119.

Tepass, U., Gruszynski-Defeo, E., Haag, T. A., Omatyar, L., Torok, T., and Hartenstien, V. (1996). Shotgun encodes *Drosophila* E-cadherin and is preferentially required during cell rearrangement in the neuroectoderm and other morphogenetically active epithelia. *Genes Dev.* **10** (6), 672–685.

Terns, R. M., Kroll-Conner, P., Zhu, J., Chung, S., and Rothman, J. H. (1997). A deficiency screen for zygotic loci required for establishment and patterning of the epidermis in *Caenorhabditis elegans. Genetics* **146**(I), 185–206.

Williams-Masson, E. M., Malik, A. N., and Hardin, J. (1997). An actin-mediated two-step mechanism is required for ventral enclosure of the *C. elegans* hypodermis. *Development.* **124,** 2889–2901.

Wilson, P. A., and Keller, R. E. (1991). Cell rearrangement during gastrulation of *Xenopus*: Direct observation of cultured explants. *Development* **105,** 155–166.

Received for publication April 20, 1998
Revised August 4, 1998
Accepted August 4, 1998